Target recognition based on phase noise of received laser signal in lidar jammer

Mahdi Nouri, Mohsen Mivehchy*, and Mohamad Farzan Sabahi

Department of Electrical Engineering, University of Isfahan, Isfahan, Iran

**Corresponding author: mivehchy@eng.ui.ac.ir*

Received March 22, 2017; accepted June 6, 2017; posted online July 11, 2017

In this Letter, a method based on the effects of imperfect oscillators in lasers is proposed to distinguish targets in continuous wave tracking lidar. This technique is based on the fact that each lidar signal source has a specific influence on the phase noise that makes real targets from the false ones. A simulated signal is produced by complex circuits, modulators, memory, and signal oscillators. For example, a deception laser beam has an unequal and variable phase noise from a real target. Thus, the phase noise of transmitted and received signals does not have the same power levels and patterns. To consider the performance of the suggested method, the probability of detection (P_D) is shown for various signal-to-noise ratios and signal-to-jammer ratios based on experimental outcomes.

OCIS codes: 030.5630, 050.5080, 060.5625, 070.1170, 070.6020.

doi: 10.3788/COL201715.100302.

Nowadays, coherent Doppler tracking lidars are extensively used due to their low required signal power in velocity and range measuring of moving targets[1–5]. Idyllically, a speckle noise free signal with Doppler frequency can be denoted with a spectral frequency line[6]. A narrower linewidth laser source with linear frequency-modulated continuous-wave (LFMCW) modulation is extensively employed in several applications. Particularly, when the accurate velocity and range is required in the lidar system[7–10]. To confuse the tracking lidars, deception laser beam (DLB) systems are used to produce false signals by storage, velocity and distance of signal processing, and sending back the lidar and radar signal[11]. In a DLB system, the input laser beam (LB) signal is first downconverted to an intermediate frequency (IF) by a laser local oscillator (LO) in a coupler. Then, an analog-to-digital converter (ADC) quantizes and samples these IF signals. Then, they are rescheduled to produce the DLB signal properties like amplitude, frequency, and phase. After digital-to-analog conversion (DAC), the fake signal is upconverted by the LO signal with a false Doppler frequency, through a single-sideband (SSB) modulator, to send back to a hostile transmitter[12–14]. The DLB recognition is one of the serious problems of tracking lidar systems. The authors in Ref. [15] proposed an arbitrarily phase-coded method that could be utilized to decline the replicas. Some techniques focus on the characteristics of the lidar signal. One of these techniques is proposing a cone class to categorize the DLB signals based on the number of DAC quantization levels[16]. Another method[17] utilizes a support vector machine (SVM) with kernel linear discriminator analysis (KLDA) feature extraction to separate the targets.

In this Letter, a discrimination method is proposed to recognize the beat frequency signal (BFS) generated by a DLB that has a higher−order nonlinearity (phase noise) of transmitting light from false signals. This method concentrates on various phase noise levels of the DLB block and a hostile lidar. In a CW tracking lidar, the master oscillator (MO) produces the lidar signal due to its own phase noise. In other words, this signal is signified with particular phase noise characteristics by the laser oscillator. The MO of tracking lidars has low-phase noise level oscillators. On the other hand, the DLB jammer has a high−phase noise level since several kinds of subsystems exist in the DLB structure. A simulated DLB signal made through complex circuits has higher phase noise levels and diverse patterns in comparison to a real signal target. It should be noted that the power spectrum of the phase noise is measured by the same set of circuits.

The CW transmitted signal with laser frequency modulation (LFM) can be expressed as

$$x(t) = \sqrt{E_s}e^{j[2\pi f_c t+\pi\mu t^2+\varphi_{\mathrm{MO}}(t)]}, \tag{1}$$

where E_s, f_c, μ, and $\varphi_{\mathrm{MO}}(t)$ are the lidar signal power, the lidar central frequency, the frequency chirp rate, and the instantaneous phase of the MO of lidar, respectively. The received real and DLB signal in the IF band can be written as

$$y_\varphi(t) = \begin{cases} \sqrt{E_s}\tilde{a}_r \exp\{j[2\pi(f_{\mathrm{IF}}+f_{d_r})t+\pi\mu t^2+2\pi\mu\tau_r t+\varphi_{\mathrm{MO}}(t-\tau_r)-\varphi^r_{\mathrm{LO}}(t)]\}+\nu(t)\text{: Real Target,} \\ \sqrt{E_J}\tilde{a}_J \exp\{j[2\pi(f_{\mathrm{IF}}+f_{d_J})t+\pi\mu t^2+2\pi\mu\tau_J t+\varphi_{\mathrm{MO}}(t-\tau_\delta-\tau_J)-\varphi^J_{\mathrm{LO}}(t-\tau_f)+\varphi^J_{\mathrm{LO}}(t-\tau_J)-\varphi_{\mathrm{LO}}(t)]\}+\nu(t)\text{: DLB,} \end{cases} \tag{2}$$

where $\tilde{a}_r$ and $\tilde{a}_J$ are the lidar target cross sections that have a complex Gaussian distribution with zero mean, and $2\sigma^2_{a_r}$ and $2\sigma^2_{a_J}$ variances, respectively. τ_r and τ_J denote the time delay of the real and DLB signal targets, and τ_f is $\tau_J - \tau_\delta$, which is the time delay due to distance of the lidar and DLB, and τ_δ is the delay line of the lidar receiver to calculate the phase noise in the frequency discriminator setup. The Doppler frequency of the real and DLB signal targets are displayed by f_{d_r} and f_{d_J}, and f_{IF} is the IF frequency. Moreover, $\nu(t)$ is the bandpass filtered complex additive white gain noise with zero mean and variance σ_0^2 in the IF band.

A real experimental setup, including a real DLB block and lidar system, is provided to consider the performance of the proposed technique. Figure 1 investigates the block diagram of this setup. A soft limiter is applied to decrease the effects of amplitude fluctuation and normalization, and low frequencies are filtered by a bandpass filter (BPF). Let $\delta\varphi_r(t,\tau_r) = \varphi_{\mathrm{MO}}(t-\tau_r) - \varphi^r_{\mathrm{LO}}(t)$ and $\delta\varphi_J(t,\tau_{J,f}) = \delta\varphi^J_r(t,\tau_\delta+\tau_J) + \delta\varphi^J_{\mathrm{LO}}(t,\tau_f-\tau_J)$ denote the phase noise related to the real target and DLB signals, respectively, where $\delta\varphi^J_r(t,\tau_\delta+\tau_J) = \varphi_{\mathrm{MO}}(t-\tau_\delta-\tau_J) - \varphi^r_{\mathrm{LO}}(t)$ and $\delta\varphi^J_{\mathrm{LO}}(t,\tau_f-\tau_J) = \varphi^J_{\mathrm{LO}}(t-\tau_J) - \varphi^J_{\mathrm{LO}}(t-\tau_f)$. It can be expressed that the terms $\varphi_{\mathrm{MO}}(t)$ and $\varphi^r_{\mathrm{LO}}(t)$ are the instantaneous phase related to the MO and LO of the lidar receiver. On the other hand, $\varphi^J_{\mathrm{LO}}(t)$ is the instantaneous phase of the LO of the DLB oscillator. For the real oscillators, it can be assumed that $\delta\varphi_r(t,\tau_r) \ll 1$. Therefore, by ignoring some small terms, we have

$$y_\varphi(t) = \begin{cases} j[\tau_r\delta\varphi_r(t,\tau_r) + \pi\mu t^2]e^{j[2\pi(f_{\mathrm{IF}}+f_{d_r})t]} \\ \quad +\nu(t)\text{:Real Target}, \\ j\{\tau_{J,f}[\delta\varphi^J_r(t,\tau_\delta+\tau_J) + \delta\varphi^J_{\mathrm{LO}}(t,\tau_{J,f})] + \pi\mu t^2\} \\ \quad e^{j[2\pi(f_{\mathrm{IF}}+f_{d_J})t]} + \nu(t)\text{:DLB}. \end{cases} \tag{3}$$

Note that $\delta\varphi_J(t,\tau_{J,f})$ consists of two sections. The first term is $\delta\varphi^J_r(t,\tau_\delta+\tau_J)$, related to lidar phase noise, and the second term is $\delta\varphi^J_{\mathrm{LO}}(t,\tau_f-\tau_J)$, corresponding to DLB. It can be presumed that the noise term $\nu(t)$ is independent from phase noises. The term $\pi\mu t^2$ appears in both the real signal and the DLB signal and can be neglected. Finally, the power spectrum density (PSD) of the phase noise $S_{Y_\varphi}(f)$ is

$$S_{Y_\varphi}(f) = \begin{cases} 4\pi^2 f^2[\tau_k^2 S_{\varphi_r(t,\tau_k)}(f)] + S_v(f)\text{:Real Target}, \\ 4\pi^2 f^2[(\tau_\delta+\tau_J)^2 S_{\varphi^J_r(t,\tau_d+\tau_J)}(f) + \tau^2_{J,f} S_{\varphi_J(t,\tau_{J,f})}(f)] + S_v(f)\text{:DLB}, \end{cases} \tag{4}$$

where $S_v(f)$ represents the PSD of $\nu(t)$. Finally, the phase noise power spectrum is achieved in the [10 kHz, 1 MHz] frequency band. In the applicable lidar systems, by considering these conditions the effect of LFM is not apparent like the larger τ_δ that causes the lower noise floor and higher total phase noise power. However, increasing the delay line limits the $f_{\max}$. The phase noise power P_{s_φ} in this bandwidth $\mathrm{BW} = f_{\max} - f_{\min}$ can be written as

$$P_{s_\varphi} = 4\pi^2 A^2_{\mathrm{os}}\tau_d^2 \int_{f_{\min}}^{f_{\max}} f^2 S_{\varphi_{\mathrm{os}}}(f)\mathrm{d}f. \tag{5}$$

The term P_{Y_φ} calculated by Eq. (5) has the signal power and phase noise power in the determined bandwidth, therefore, received signals should be normalized by the lidar signal power to reduce the effects of the signal power that make the discrimination accurate. Assume that H_1 represents the real target signal hypothesis; on the other hand, H_0 shows the DLB hypothesis. The phase noise power distribution of the received signal can be achieved by the expectation value of P_{Y_φ} that depends on $E(|\tilde{a}_r|^2)$ and $E(|\tilde{a}_J|^2)$. Therefore, the normalized hypothesis test can be denoted as

$$\begin{cases} \bar{P}_{Y_\varphi} \sim H_1, \bar{P}_{Y_\varphi} \sim |\tilde{a}_r|^2 + N_W, \\ \bar{P}_{Y_\varphi} \sim H_0, \bar{P}_{Y_\varphi} \sim |\tilde{a}_J|^2\left(1 + \frac{P_J}{P_r}\right) + N_W, \end{cases} \tag{6}$$

where $N_W = \int_{f_{\min}}^{f_{\max}} N_{\mathrm{IF}}(f)\mathrm{d}f \approx \mathrm{BW}\frac{N_0}{2}$ is the noise power that adds to the signal phase noise in the measuring bandwidth. Now, different situations can be observed that may happen in this assumption. First, it can be mentioned that

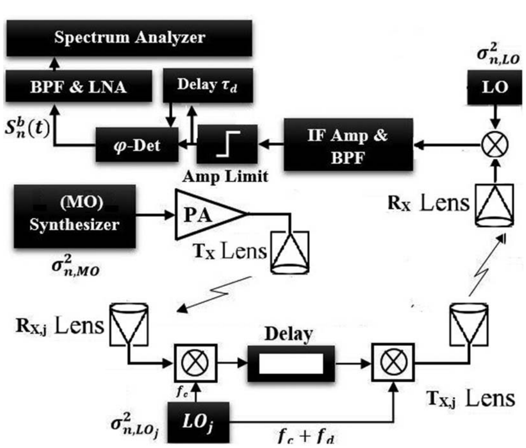

Fig. 1. Block diagram of the discrimination method to recognize the lidar signal targets based on the phase noise.

$\bar{P}_{Y_\varphi}$ has a Rician distribution with $R(\mu,\sigma)$. These parameters can be categorized as $\mu = N_W$, $\sigma_{H_1} = 1$, and $\sigma_{H_0} = \sqrt{(1+\frac{P_J}{P_r})}$. If M independent time frames are gathered in the likelihood ratio test (LRT), the hypothesis test is changed to

$$\frac{\prod_{l=1}^{M} p(P_{Y_\varphi}^l|H_1)}{\prod_{l=1}^{M} p(P_{Y_\varphi}^l|H_0)} = \frac{\prod_{l=1}^{M} \frac{P_{Y_\varphi}^l}{\sigma_{H_1}^2}\exp\left(-\frac{(P_{Y_\varphi}^l-\mu)^2}{\sigma_{H_1}^2}\right) I_0\left(\frac{\mu P_{Y_\varphi}^l}{\sigma_{H_1}^2}\right)}{\prod_{l=1}^{M} \frac{P_{Y_\varphi}^l}{\sigma_{H_0}^2}\exp\left(-\frac{(P_{Y_\varphi}^l-\mu)^2}{\sigma_{H_0}^2}\right) I_0\left(\frac{\mu P_{Y_\varphi}^l}{\sigma_{H_0}^2}\right)} \underset{H_0}{\overset{H_1}{\gtrless}} \gamma, \tag{7}$$

where $I_0(x)$ is the first kind of zero-order modified Bessel function. After some simplifications, the logarithm of Eq. (7) of the LRT becomes

$$\Lambda(P_{Y_\varphi}^l) = \sum_{l=1}^{M}\left\{\left[\frac{(\sigma_{H_1}^2-\sigma_{H_0}^2)}{\sigma_{H_1}^2\sigma_{H_0}^2}(P_{Y_\varphi}^l-\mu)^2\right]\left[\ln I_0\left(\frac{\mu P_{Y_\varphi}^l}{\sigma_{H_1}^2}\right) - \ln I_0\left(\frac{\mu P_{Y_\varphi}^l}{\sigma_{H_0}^2}\right)\right]\right\} \underset{H_0}{\overset{H_1}{\gtrless}} \ln\gamma\left(\frac{\sigma_{H_1}^2}{\sigma_{H_0}^2}\right)^M. \tag{8}$$

The SJR can investigate the difference in the received phase noise power in the lidar and DLB signals. So, we have

$$\mathrm{SJR} = \frac{|\tilde{a}_r|^2 + N_W}{|\tilde{a}_J|^2\left(1+\frac{P_J}{P_r}\right) + N_W} = \frac{\mathrm{SNR}+1}{\mathrm{JNR}\left(1+\frac{P_J}{P_r}\right)+1}, \tag{9}$$

where the jammer-to-noise ratio (JNR) is the received phase noise power of the DLB signal-to-noise level. In practical cases, the signal power of the DLB is greater than lidar; it means that JNR > SNR. However, in the equal power case, the second term in the DLB $(1+\frac{P_J}{P_r})$ has a greater quantity than the lidar signal; therefore, it can be considered for discrimination. Furthermore, if the phase noise power of the DLB was smaller than lidar, $P_J < P_r$, the total DLB signal has a greater phase noise because of two terms of the phase noise of the lidar and DLB together. By increasing the M time frames in this rare case, the DLB signal can be discriminated from the lidar signal. In fact, Eq. (8) cannot be simplified easily. Then the term $\ln I_0(x)$ can be approximated by $\frac{x^2}{4}$ when $|x| \ll 1$ and in other points by $|x|$. So, we have

$$\Lambda(P_{Y_\varphi}^l) = \sum_{l=1}^{M}\left\{\left[\frac{(\sigma_{H_1}^2-\sigma_{H_0}^2)}{\sigma_{H_1}^2\sigma_{H_0}^2}(P_{Y_\varphi}^l-\mu)^2\right]\left[\left(\frac{\mu P_{Y_\varphi}^l}{\sigma_{H_1}^2}\right)^2 - \left(\frac{\mu P_{Y_\varphi}^l}{\sigma_{H_0}^2}\right)^2\right]\right\} \underset{H_0}{\overset{H_1}{\gtrless}} \ln\gamma\left(\frac{\sigma_{H_1}^2}{\sigma_{H_0}^2}\right)^M. \tag{10}$$

Equation (8) can be solved based on $P_{Y_\phi}^l$. The appropriate solution is

$$\Lambda(P_{Y_\phi}^l) = \sum_{l=1}^{M} P_{Y_\phi}^l \underset{H_0}{\overset{H_1}{\gtrless}} \frac{1}{2}\left(\mu + \sqrt{\mu^2 + 4\sqrt{\gamma'}}\right). \tag{11}$$

Other coefficients can be absorbed into the threshold γ' of decision. The final distribution of $\Lambda(P_{Y_\varphi}^l) = \sum_{l=1}^{M} P_{Y_\varphi}^l$ can be approximated by[18]

$$\begin{aligned} &f_M(\Lambda(P_{Y_\varphi}^l)/\sqrt{M},\mu,\sigma) \\ &= \frac{1}{2\pi}\exp\left[-\frac{(\Lambda(P_{Y_\varphi}^l)/\sqrt{M}-\mu\sqrt{M})^2}{2\sigma^2}\right] \\ &\quad + \frac{a_0}{a_1}\left[\left(\frac{\Lambda(P_{Y_\varphi}^l)/\sqrt{M}-a_2}{a_1}\right)^2 - 3\right] \\ &\left(\frac{\Lambda(P_{Y_\varphi}^l)/\sqrt{M}-a_2}{a_1}\right)\exp\left(-\frac{(\Lambda(P_{Y_\varphi}^l)/\sqrt{M}-a_2)^2}{2a_1^2}\right), \end{aligned} \tag{12}$$

where the constants a_0, a_1, a_2 are attained using nonlinear least squares fitting with the exact cumulative distribution function. Then, the probability detection can be achieved by $P_D = P(\Lambda(P_{\mathrm{PN}}^l) > \gamma\,|H_1)$.

Different techniques have been proposed to measure the phase noise of an oscillator (see Ref. [19]). In this Letter, a frequency discriminator is used to measure the phase noise in the light-wave system[20–22]. In the experimental results, an optoelectronic oscillator (OEO) with two cascaded Mach–Zehnder modulators (MZMs). In optical lasers the phase noise has an approximately 12 dB higher average power than the thermal noise floor. In this test, the signal wavelength is 1550 nm, and the LFM frequency deviation is 300 MHz with a sweep rate of 1 kHz. The DLB oscillator is similar to lidar transmitter with very low-phase noise level. In this setup, the DLB receives the lidar signal and amplifies the signal via the IF amplifier. Then, the IF frequency is attained by the output of downconversion. This IF signal output goes to a 10 bit ADC, then to create an appropriate delay and amplitude comes to SPARTAN III FPGA. Then, it is converted by a 12 bit DAC to analog signal and filtered by a reconstruction filter to decline the effects of the SSB modulator, i.e., $f_{\mathrm{LO}} + f_d$, quantization, and sampling. A microcontroller is used to determine the Doppler frequency of the targets. Then, it is upconverted to the

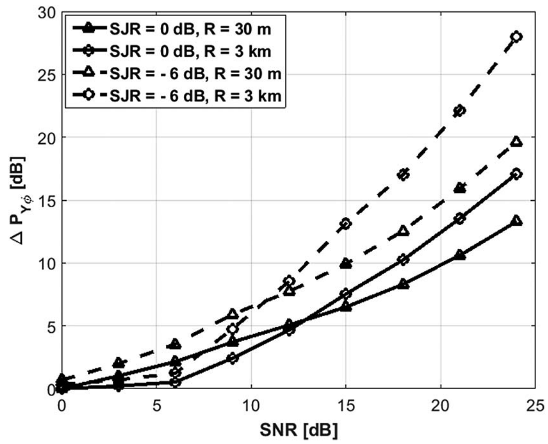

Fig. 2. ΛP_{Y_ϕ} versus SNRs and different SJRs.

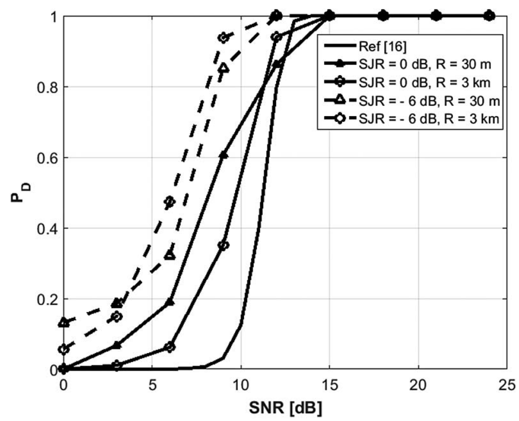

Fig. 3. Probability of detection in comparison to the method of Ref. [16] versus SNRs in different SJRs in the case of a very low false alarm.

light-wave band by a fiber coupler. This optic signal is amplified and sent back to the hostile lidar. The received lidar and DLB signals are downconverted with the coupler and filtered by a 10 kHz–1 MHz BPF to attain the phase noise power. The processing and decision time is 1 s. All achieved results are based on 100 independent tests. The range and the Doppler frequency of the DLB false target are 30 m and 50 m/s, respectively. Figure 2 shows ΛP_{Y_ϕ} in different SNRs when SJR $= 0$ and SJR $= -6$ dB, where $R = 30$ m and $R = 3$ km. As can be observed, ΛP_{Y_ϕ} for a near distance for low SNRs is greater than $R = 3$ km, however when the SNR is enhanced the phase noise power is increased because of a greater time delay, which makes the phase noise higher than $R = 30$ m. When the SNR > 9 dB, the difference is high enough to discriminate targets. Figure 3 demonstrates the P_D versus the SNR in comparison to Ref. [6] for SJR $= 0$ and SJR $= -6$ dB, where $R = 30$ m and $R = 3$ km, respectively. It shows that a greater DLB signal power causes a more accurate detection ($P_D > 90\%$), and, furthermore, a longer distance $R = 3$ km in higher SNRs make better detectors.

In this Letter, a new method is proposed to discriminate real and DLB targets in a CW tracking lidar based upon an altered phase noise power of the received lidar signal. The DLB signal is produced through an SSB modulator and another LO that caused a greater phase noise than the received lidar signal of the real targets. An adjustable structure is employed to consider the performance of the proposed phase noise method at near and far distances with different SJRs in an operational DLB system. The experimental outcomes indicate that the proposed method can discriminate the DLB signals from real targets with a great amount of P_D, exactly when the SNR > 10 dB, and for a higher DLB power (SJR < 0) the proposed method gives a better P_D.

References

1. L. Lu, J. Yang, L. Zhai, R. Wang, Z. Cao, and B. Yu, Opt. Express **20**, 8598 (2012).
2. R. S. Matharu, J. Perchoux, R. Kliese, Y. L. Lim, and A. D. Rakic, Opt. Lett. **36**, 3690 (2011).
3. B. Ruth, Opt. Laser Technol. **19**, 83 (1987).
4. G. Giuliani, M. Norgia, S. Donati, and T. Bosch, J. Opt. A **4**, S283 (2002).
5. L. Scalise, Y. Yu, G. Giuliani, G. Plantier, and T. Bosch, IEEE Trans. Instrum. Meas. **53**, 223 (2004).
6. R. N. Bracewell, "The basic theorems," in *The Fourier Transform and Its Applications* (McGraw Hill, 2000), Chap. 6.
7. L. T. Wang, K. Iiyama, F. Tsukada, N. Yoshida, and K.-I. Hayashi, Opt. Lett. **18**, 1095 (1993).
8. R. Agishev, B. Gross, F. Moshary, A. Gilerson, and S. Ahmed, Appl. Phys. B **85**, 149 (2006).
9. Z. Ma, C. Zhang, P. Ou, G. Luo, and Z. Zhang, Chin. Opt. Lett. **6**, 261 (2008).
10. S. J. Roome, Electron. Commun. Eng. J. **2**, 147 (1990).
11. D. Gold and H. Ur, Electron. Lett. **29**, 411 (1993).
12. K. Iiyama, L.-T. Wang, and K. Hayashi, J. Lightwave Technol. **14**, 173 (1996).
13. M.-C. Amann, T. Bosch, M. Lescure, R. Myllyla, and M. Rioux, Opt. Eng. **40**, 10 (2001).
14. S. D. Berger, IEEE Trans. Aerosp. Electron. Syst. **39**, 725 (2003).
15. J. Zhang, X. Zhu, and H. Wang, Electron. Lett. **45**, 1052 (2009).
16. M. Greco, F. Gini, and A. Farina, IEEE Trans. Signal Process. **56**, 1984 (2008).
17. M. Nouri, M. Mivehchy, and S. A. Aghdam, in *IEEE 6th International Conference on Computing Communication and Networking Technologies (ICCCNT)* (2015), p. 1.
18. J. A. Lopez-Salcedo, IEEE Signal Process. Lett. **16**, 153 (2009).
19. H. Gheidi and A. Banai, IEEE Trans. Microwave Theory Tech. **58**, 468 (2010).
20. D. Eliyahu, D. Seidel, and L. Maleki, IEEE Trans. Microwave Theory Tech. **56**, 449 (2008).
21. K. H. Lee, J. Y. Kim, and W. Y. Choi, IEEE Photon. Technol. Lett. **19**, 1982 (2007).
22. L. Zhang, A. Poddar, U. Rohde, and A. Daryoush, IEEE Photon. J. **5** (2013).